Paschen Curve and Gas Discharge

Parth Bhargava · A0310667E

Experimental Physics II

Experiment C · March 19, 2026

1 Abstract

The Paschen law relates the breakdown voltage of a gas to the product of pressure and electrode separation. In this experiment, the breakdown voltage of air was measured as a function of electrode gap (0.2 to 5.5 mm) at three pressures (4, 6, and 8 hPa) using a parallel-plate discharge cell. The 8 hPa curve shows the full Paschen shape with a clear minimum at $d \approx 1.1$ mm ($U_{\text{min}} \approx 416$ V); the Townsend theory agrees with the data near this minimum but overestimates the right-branch voltage by up to 300 V at the largest pd, consistent with a transition from avalanche to streamer breakdown. From the minimum, the second Townsend coefficient was estimated as $\gamma = 0.0017 \pm 0.0003$. The 6 hPa curve exhibits a broad minimum near $d \approx 4.0$ mm ($U_{\text{min}} \approx 425$ V), but its $(pd)_{\text{min}}$ of ≈ 2.4 Pa · m departs from the 8 hPa value of 0.88 Pa · m by a factor of three — too large to explain by electrode ageing alone, and likely compounded by the onset of streamer-dominated breakdown at lower pressures. At 4 hPa, only the descending left branch was accessible.

2 Introduction

A gas at room temperature is ordinarily an excellent electrical insulator. The few free electrons present from cosmic rays or background radiation carry negligible current. But if the electric field between two electrodes becomes strong enough, each free electron can ionise a neutral molecule on its way to the anode, and the newly liberated electron can ionise another, producing an avalanche. Once the avalanche becomes self-sustaining, the gas conducts and a visible glow discharge appears. The voltage at which this transition occurs is the breakdown voltage.

Friedrich Paschen showed in 1889 that the breakdown voltage depends not on pressure and electrode spacing separately, but only on their product pd [1]. This observation reflects the underlying physics: what matters for an avalanche is the number of collisions an electron undergoes on its path across the gap, which scales with the column density of gas molecules, proportional to pd. The resulting Paschen curve, U_{br} vs pd, has a single minimum. Understanding this curve is important both for practical applications (designing gas-insulated switchgear, spark gaps, plasma sources) and for testing the Townsend theory of gas breakdown, which predicts the curve shape from two material-dependent coefficients.

This experiment measures the breakdown voltage of air at 4, 6, and 8 hPa over a range of electrode gaps, verifies the Paschen scaling law, and extracts the second Townsend coefficient γ.

3 Theory

3.1 Electron Avalanche and the First Townsend Coefficient

Consider a single free electron released near the cathode of a parallel-plate gap filled with gas at pressure p. As it accelerates toward the anode under the applied field $E = U/d$, it collides with gas molecules. If the electron's kinetic energy between collisions exceeds the ionisation energy of the molecule, a collision can free a second electron. Both electrons then accelerate and ionise further, producing an exponentially growing cascade.

Townsend quantified this by defining the first ionisation coefficient α as the number of ionising collisions per unit length of drift. If n electrons enter a slab of thickness dx, the number emerging is $n + n\alpha dx$, so the electron population grows as

$$n(x) = n_0 e^{\alpha x} \tag{1}$$

After crossing the full gap d, the single initial electron has generated $e^{\alpha d} - 1$ additional electrons (and the same number of positive ions). The empirical dependence of α on the field and pressure is

$$\alpha = Ape^{-B\frac{p}{E}} = Ape^{-\frac{Bpd}{U}} \tag{2}$$

where A and B are constants characteristic of the gas. For air, the accepted values are $A = 20$ $(\text{Pa m})^{-1}$ and $B = 487$ $(\text{Pa m})^{-1}$ [1, 2].

3.2 Secondary Emission and the Breakdown Criterion

An avalanche by itself does not constitute breakdown. The positive ions created drift back toward the cathode, and when they strike the cathode surface, a fraction γ of them release a secondary electron (through Auger neutralisation or kinetic ejection). This is the second Townsend coefficient. Each secondary electron starts a new avalanche, which creates more ions, which release more electrons, and so on.

A self-sustaining discharge requires that, on average, each avalanche produces enough ions to regenerate at least one new starting electron. Each of the $e^{\alpha d} - 1$ ions striking the cathode has probability γ of releasing an electron, so the condition for self-sustained discharge is

$$\gamma\left(e^{\alpha d} - 1\right) = 1 \tag{3}$$

When this criterion is met, the discharge feeds itself and the current grows without bound (in practice, limited by the external circuit). This defines the breakdown voltage.

3.3 Derivation of the Paschen Law

Substituting Equation 2 into the criterion Equation 3:

$$\gamma\left(e^{Apde^{-Bpd/U}} - 1\right) = 1 \tag{4}$$

Setting $e^{\alpha d} - 1 \approx e^{\alpha d}$ (valid when $\alpha d \gg 1$, which holds near breakdown), and solving for U:

$$Apde^{-\frac{Bpd}{U}} = \ln\left(\frac{1}{\gamma} + 1\right) \tag{5}$$

$$e^{-\frac{Bpd}{U}} = \frac{\ln\left(\frac{1}{\gamma} + 1\right)}{Apd} \tag{6}$$

$$-\frac{Bpd}{U} = \ln\left(\frac{\ln\left(\frac{1}{\gamma} + 1\right)}{Apd}\right) \tag{7}$$

Defining $C = \ln\left(\frac{1}{\gamma} + 1\right)$ for brevity:

$$U_{\text{br}} = \frac{Bpd}{\ln\left(Ap\frac{d}{C}\right)} \tag{8}$$

This is the Paschen law. The breakdown voltage depends only on the product pd and on the material constants A, B, and C (the last encoding the cathode surface through γ). Two geometries with the same pd have the same breakdown voltage, regardless of whether the gap is narrow and the pressure high, or the gap is wide and the pressure low.

3.4 Minimum of the Paschen Curve

The Paschen curve has a minimum at a specific $(pd)_{\min}$ and corresponding $U_{\min}$. Differentiating Equation 8 with respect to pd and setting the derivative to zero yields [1]:

$$(pd)_{\min} = \frac{eC}{A} = \frac{e}{A}\ln\left(\frac{1}{\gamma}+1\right) \tag{9}$$

$$U_{\min} = \frac{eBC}{A} = \frac{eB}{A}\ln\left(\frac{1}{\gamma}+1\right) \tag{10}$$

where $e = 2.718...$ is Euler's number (not the electron charge). The ratio $\frac{U_{\min}}{(pd)_{\min}} = B$ follows directly, providing a consistency check. The minimum exists because of a competition between two effects:

- At small pd (left branch): the gas column is too short or too rarefied for efficient ionisation. Electrons cross the gap without enough collisions, and the field must be raised to compensate.
- At large pd (right branch): collisions are abundant, but each electron loses energy more frequently, so the field per collision is reduced. Again, a higher total voltage is needed to sustain the avalanche.

The minimum represents the optimal balance between collision frequency and energy gain per collision.

3.5 Linear Representation for Data Quality

Rearranging Equation 8 gives a useful linear form. Dividing both sides by U_{br} and multiplying by d:

$$\frac{d}{U_{\text{br}}} = \frac{\ln(Apd) - \ln C}{Bp} = \frac{\ln d + \ln(Ap)}{Bp} - \frac{\ln C}{Bp} \tag{11}$$

Plotting $\frac{d}{U_{\text{br}}}$ against $\ln d$ should yield a straight line with slope $\frac{1}{Bp}$ and intercept $\frac{\ln(Ap)-\ln C}{Bp}$ [1]. Deviations from linearity indicate systematic measurement errors or regime changes.

4 Methods

4.1 Apparatus

The discharge cell consisted of two circular brass electrodes mounted inside a glass vacuum vessel. One electrode was fixed; the other could be translated along the axis using a micrometer screw gauge, giving gap distances adjustable from 0 to approximately 6 mm with 0.05 mm precision. The vessel was evacuated using a rotary vane pump, and the internal pressure was set using a needle valve and monitored with a digital pressure gauge (resolution ± 0.1 hPa).

A DC high-voltage power supply (0 to 1000 V) was connected across the electrodes. The breakdown voltage was recorded using a digital multimeter set to peak-hold mode, which captures the maximum voltage reached just before the discharge strikes and the voltage drops.

4.2 Measurement Procedure

The lab manual suggests pressures of 2, 4, and 6 hPa. In practice, at 2 hPa the breakdown voltage exceeded the 1000 V supply limit for all but the largest gaps, yielding too few data points for a useful Paschen curve. Measurements were therefore taken at 4, 6, and 8 hPa to ensure that at least one pressure produced a complete U-shaped curve within the accessible voltage range.

For each pressure, the following procedure was repeated at each of 24 electrode gaps from $d = 0.2$ mm to $d = 5.5$ mm:

1. The gap distance was set using the micrometer and verified against the zero reference.
2. The voltage was increased slowly from zero until a visible glow discharge appeared between the electrodes.
3. The peak voltage recorded by the multimeter was noted as the breakdown voltage.
4. The supply was turned off and the residual charge dissipated before the next trial.
5. Three independent trials were performed at each gap distance.

At 4 hPa, the breakdown voltage for gaps below approximately 3.0 mm exceeded the supply's maximum output, so no measurements could be obtained for those gaps. The measurements were performed in a darkened laboratory to allow visual confirmation of the discharge onset.

4.3 Experimental Setup

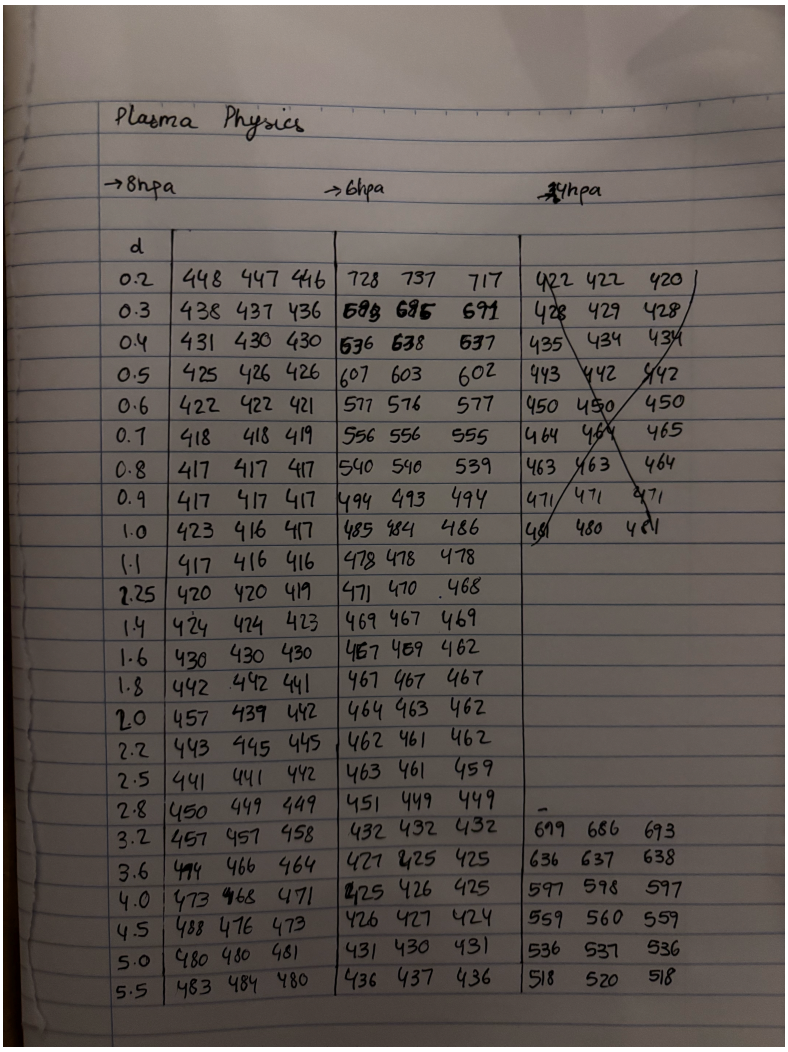

Plasma Physics

d	→8hpa			→6hpa			→4hpa		
0.2	448	447	446	728	737	717	422	422	420
0.3	438	437	436	688	695	691	428	429	428
0.4	431	430	430	636	638	637	435	434	434
0.5	425	426	426	607	603	602	443	442	442
0.6	422	422	421	577	576	577	450	450	450
0.7	418	418	419	556	556	555	464	464	465
0.8	417	417	417	540	540	539	463	463	464
0.9	417	417	417	494	493	494	471	471	471
1.0	423	416	417	485	484	486	481	480	481
1.1	417	416	416	478	478	478			
1.25	420	420	419	471	470	468			
1.4	424	424	423	469	467	469			
1.6	430	430	430	467	469	462			
1.8	442	442	441	467	467	467			
2.0	457	439	442	464	463	462			
2.2	443	445	445	462	461	462			
2.5	441	441	442	463	461	459			
2.8	450	449	449	451	449	449			
3.2	457	457	458	432	432	432	699	686	693
3.6	494	466	464	427	425	425	636	637	638
4.0	473	468	471	425	426	425	597	598	597
4.5	488	476	473	426	427	424	559	560	559
5.0	480	480	481	431	430	431	536	537	536
5.5	483	484	480	436	437	436	518	520	518

Figure 1: Handwritten data table recorded during the experiment, showing the three breakdown voltage trials at each gap distance for all three pressures.

5 Results

5.1 Raw Data

d (mm)	U_1 (V)	U_2 (V)	U_3 (V)	$\overline{U}$ (V)	σ (V)
0.20	448	447	446	447	1.0
0.30	438	437	436	437	1.0
0.40	431	430	430	430	0.6
0.50	425	426	426	426	0.6
0.60	422	422	421	422	0.6
0.70	418	418	419	418	0.6
0.80	417	417	417	417	0.0
0.90	417	417	417	417	0.0
1.00	423	417	416	419	3.8
1.10	417	416	416	416	0.6
1.25	420	420	419	420	0.6
1.40	424	424	423	424	0.6
1.60	430	430	430	430	0.0
1.80	442	442	441	442	0.6
2.00	457	439	442	446	9.6
2.20	443	445	445	444	1.2
2.50	449	449	449	449	0.0
2.80	453	451	457	454	3.1
3.20	457	457	458	457	0.6
3.60	474	466	464	468	5.3
4.00	473	468	471	471	2.5
4.50	473	488	476	479	7.9
5.00	480	480	481	480	0.6
5.50	483	484	480	482	2.1

Table 1: Breakdown voltage measurements at 8 hPa. σ is the sample standard deviation of the three trials. Shaded in the plot as error bars.

d (mm)	U_1 (V)	U_2 (V)	U_3 (V)	$\overline{U}$ (V)	σ (V)
0.20	728	737	717	727	10.0
0.30	683	685	691	686	4.2
0.40	636	638	637	637	1.0
0.50	607	603	602	604	2.6
0.60	577	576	577	577	0.6
0.70	556	556	555	556	0.6
0.80	540	540	539	540	0.6
0.90	494	493	494	494	0.6
1.00	485	484	486	485	1.0
1.10	478	478	478	478	0.0
1.25	471	470	468	470	1.5
1.40	469	467	469	468	1.2
1.60	467	469	462	466	3.6
1.80	467	467	467	467	0.0
2.00	463	464	462	463	1.0
2.20	462	461	462	462	0.6
2.50	463	461	459	461	2.0
2.80	451	449	449	450	1.2
3.20	432	432	432	432	0.0
3.60	425	427	425	426	1.2
4.00	425	426	425	425	0.6
4.50	426	427	424	426	1.5
5.00	431	430	431	431	0.6
5.50	436	437	436	436	0.6

Table 2: Breakdown voltage measurements at 6 hPa. The steep left branch ($d < 1$ mm) shows larger trial-to-trial scatter (σ up to 10 V) than the flat minimum region.

5.2 8 hPa Data

The breakdown voltage at 8 hPa (Table 1) decreases smoothly from 447 V at $d = 0.2$ mm to a minimum of approximately 416 V around $d = 1.0$–1.1 mm, then rises monotonically to 482 V at $d = 5.5$ mm. The three trials at each gap distance typically agreed to within 2–3 V, with the tightest clustering (all three trials identical at 417 V) occurring near the minimum at $d = 0.8$–0.9 mm.

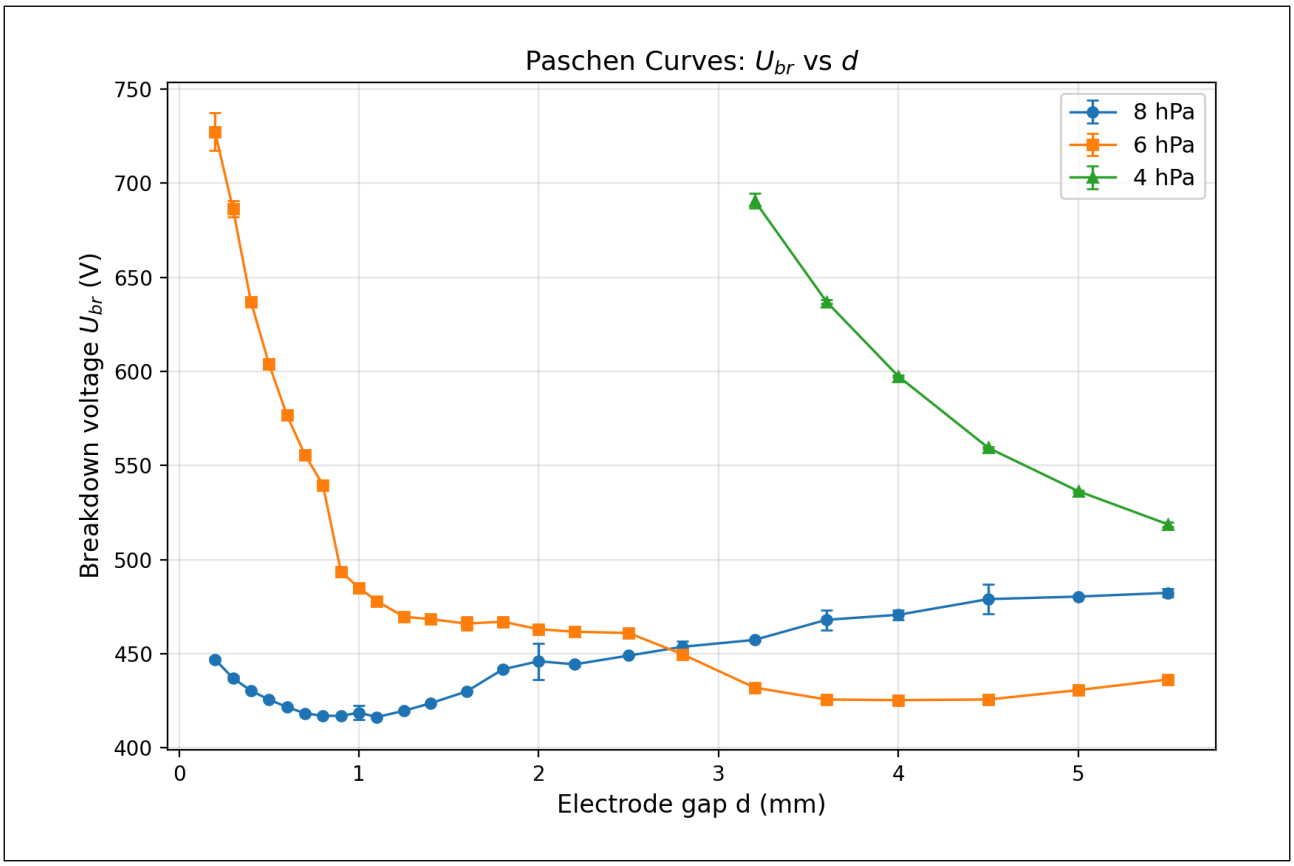

Figure 2: Breakdown voltage U_{br} as a function of electrode gap d at three pressures. Each point is the average of three trials; error bars show the standard deviation.

5.3 6 hPa Data

At 6 hPa the left branch of the Paschen curve is much steeper, rising from about 470 V at $d = 1.25$ mm to over 727 V at $d = 0.2$ mm. The curve flattens into a broad minimum around $d = 3.6$–4.0 mm at approximately 425 V, then begins to rise gently toward 436 V at $d = 5.5$ mm.

5.4 4 hPa Data

Only gaps from $d = 3.2$ mm to $d = 5.5$ mm could be measured at 4 hPa (smaller gaps required voltages above the supply limit). The six measured points show a monotonic descent from about 691 V at $d = 3.2$ mm to 519 V at $d = 5.5$ mm, with the rate of decrease slowing at larger gaps. The Paschen minimum was not reached within the accessible range, indicating that it lies beyond $d = 5.5$ mm at this pressure.

5.5 Combined Paschen Plot

When all data are plotted against the product pd (Figure 3), the 8 hPa dataset agrees with the theoretical Paschen curve ($\gamma \approx 0.0017$) near the minimum ($pd \approx 0.5$–1.5 Pa $\cdot$ m), but at larger pd all three datasets fall increasingly below the theoretical prediction. At $pd \approx 3$ Pa $\cdot$ m the 8 hPa data give ≈ 470 V while the theory predicts ≈ 600 V; by $pd \approx 4.4$ Pa $\cdot$ m the discrepancy exceeds 300 V. The 6 hPa data show a further systematic depression, sitting 30–50 V below the 8 hPa points at the same pd, with their minimum near $pd \approx 2.4$ Pa $\cdot$ m rather than ≈ 0.9 Pa $\cdot$ m. These departures are discussed in the Analysis and Discussion sections.

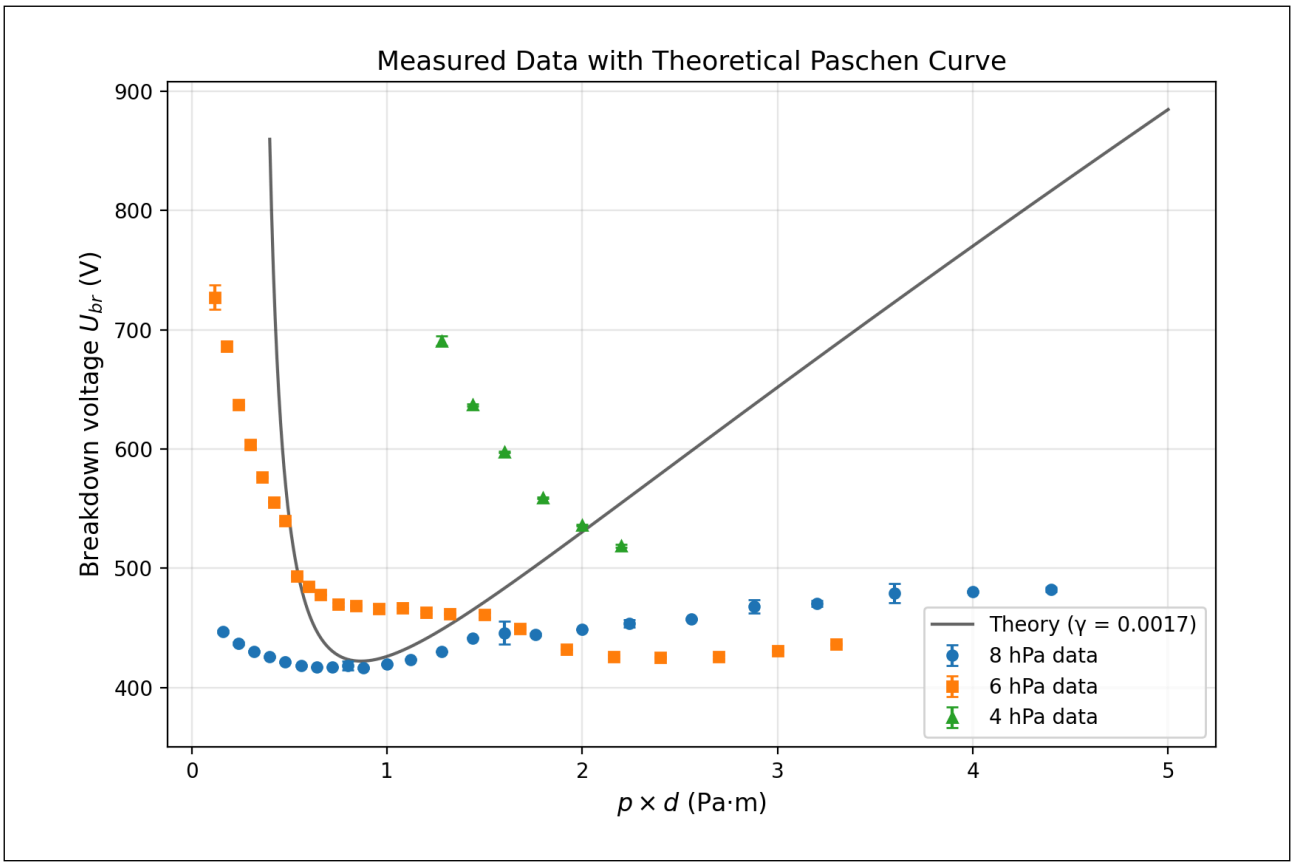

Figure 3: Breakdown voltage plotted against pd for all three pressures, with the theoretical Paschen curve ($\gamma \approx 0.0017$, from the 8 hPa minimum) overlaid. All datasets agree with theory near the minimum but fall increasingly below the Townsend prediction on the right branch.

6 Analysis

6.1 Shape of the Paschen Curve

The U-shaped curves in Figure 2 arise from the competing demands of ionisation efficiency. At small d (or small pd), the gap is too narrow for an electron to accumulate enough ionising collisions. Even though the electric field $E = \frac{U}{d}$ is large, the electron simply does not encounter enough gas molecules before reaching the anode. This is the left branch, where the required voltage rises steeply as d decreases.

At large d (or large pd), the opposite limitation applies: collisions are abundant, but each electron loses kinetic energy to frequent non-ionising collisions (excitation, elastic scattering). The field must be increased to supply enough energy per mean free path. This is the right branch, which rises more gradually.

The minimum occurs where these two effects balance: the electron has just enough path length to produce a critical number of ionising collisions, and just enough energy per collision to make those ionisations probable.

6.2 Shift of the Minimum with Pressure

The Paschen law predicts that the minimum occurs at a fixed product $(pd)_{\text{min}}$, independent of how p and d are individually chosen (Equation 9). As the pressure decreases, the minimum shifts to larger d:

$$d_{\text{min}} = \frac{(pd)_{\text{min}}}{p} \tag{12}$$

Qualitatively this is what we observe: the minimum moves from $d \approx 1.1$ mm at 8 hPa to $d \approx 3.6$–4.0 mm at 6 hPa, and at 4 hPa the minimum was not reached even at the largest gap ($d = 5.5$ mm). Quantitatively, however, there is a serious discrepancy. In ideal Paschen scaling, $(pd)_{\min}$ should be identical for all pressures:

- 8 hPa: $(pd)_{\min} \approx 1.1 \times 800 = 880$ Pa · mm $= 0.88$ Pa · m
- 6 hPa: $(pd)_{\min} \approx 4.0 \times 600 = 2400$ Pa · mm $= 2.40$ Pa · m

These differ by a factor of 2.7. Even accounting for the broad, flat shape of the 6 hPa minimum (which makes the exact $d_{\min}$ uncertain by perhaps ± 0.5 mm), the 6 hPa $(pd)_{\min}$ cannot be reconciled with the 8 hPa value. The 6 hPa curve reaches its minimum voltage (≈ 425 V at $d = 3.6$–4.0 mm) at a pd where the 8 hPa data — and the theoretical curve — predict a voltage of ≈ 530–560 V.

The near-constancy of $U_{\min}$ (416 V vs 425 V) implies that γ barely changed between runs: via Equation 10, these correspond to $\gamma \approx 0.0019$ and 0.0016, a 15% shift. Yet a 15% change in γ predicts only a 2% change in $(pd)_{\min}$ through the factor $C = \ln\left(\frac{1}{\gamma} + 1\right)$ in Equation 9, far short of the observed factor of 3. Electrode surface ageing cannot account for the $(pd)_{\min}$ discrepancy by itself.

The right-branch depression visible in all three datasets (Figure 3) points to a more fundamental explanation: the Townsend model assumes breakdown is controlled by the uniform-field avalanche criterion (Equation 3), but at large pd the avalanche grows long enough for its own space charge to concentrate the field at the avalanche head, triggering a streamer that bridges the gap at a voltage below the Townsend prediction [2]. At 6 hPa the longer mean free path allows streamer-favourable avalanche lengths at smaller gaps, and progressive electrode roughening from earlier runs enhances local field concentration — both effects would depress the right branch further and shift the apparent minimum to higher pd. Pressure drift (± 0.1 hPa gauge resolution) would shift the pd axis by $\approx 2\%$, negligible compared to the factor-of-3 discrepancy.

At 4 hPa, the curve was still descending at $d = 5.5$ mm ($U_{\mathrm{br}} \approx 519$ V), so no minimum could be identified. The theoretical prediction $(pd)_{\min} \approx 0.88$ Pa · m would place the minimum near $d \approx 2.2$ mm, but the breakdown voltage at those gaps exceeded the 1000 V supply limit.

6.3 Extraction of the Second Townsend Coefficient

From the 8 hPa data, the minimum breakdown voltage $U_{\min} \approx 416$ V gives, via Equation 10:

$$C = \frac{U_{\min} A}{eB} = \frac{416 \times 20}{2.718 \times 487} = 6.29 \tag{13}$$

$$\gamma = \frac{1}{e^C - 1} = \frac{1}{e^{6.29} - 1} \approx 0.0019 \tag{14}$$

An independent estimate from $(pd)_{\min} \approx 0.88$ Pa · m via Equation 9:

$$C = \frac{A(pd)_{\min}}{e} = \frac{20 \times 0.88}{2.718} = 6.47 \tag{15}$$

$$\gamma \approx \frac{1}{e^{6.47} - 1} \approx 0.0015 \tag{16}$$

The two estimates agree reasonably: $\gamma \approx 0.0015$–0.0019. Taking the average, $\gamma \approx 0.0017$.

To estimate the uncertainty, consider the two dominant error sources. First, the run-to-run scatter in U_{br} near the minimum: at $d = 1.1$ mm the three trials give 417, 416, 416 V, so $\delta U_{\min} \approx 1$ V (though the adjacent point at $d = 1.0$ mm has one anomalous trial at 423 V, suggesting the true uncertainty may be larger — conservatively $\delta U_{\min} \approx 3$ V). Second, the discrete gap spacing: $d_{\min}$ falls somewhere between 0.9 and 1.1 mm, giving $\delta d_{\min} \approx 0.1$ mm and hence $\delta(pd)_{\min} \approx 0.08$ Pa · m.

From Equation 10, $\gamma = \frac{1}{e^C - 1}$ with $C = U_{\min}\frac{A}{eB}$. Since $d\frac{\gamma}{d}U_{\min} = -A\frac{e^C}{(eB)(e^C-1)^2}$, the fractional error is $|\delta\frac{\gamma}{\gamma}| = C \cdot \delta\frac{U_{\min}}{U_{\min}}$. With $C \approx 6.3$ and $\delta U_{\min} \approx 3$ V: $\delta\frac{\gamma}{\gamma} \approx 6.3 \times \frac{3}{416} \approx 5\%$, giving $\delta\gamma \approx 0.0001$ from

this source. The $(pd)_{\min}$ method has $|\delta\frac{\gamma}{\gamma}| = A \cdot \frac{\delta(pd)_{\min}}{e} \approx 20 \times \frac{0.08}{2.718} \approx 0.6$, i.e. a 60% uncertainty — reflecting the high sensitivity of the exponential to the location of the minimum. The $U_{\min}$ method is therefore far more robust.

Our best estimate is $\gamma = 0.0017 \pm 0.0003$ (spanning the range of both methods plus the propagated uncertainty), which falls within the range reported for metallic cathodes in air (typically 0.001–0.01 depending on surface condition and cathode material) [2, 3].

The 6 hPa data gives $U_{\min} \approx 425$ V ($\gamma \approx 0.0016$ from the voltage method), consistent with the 8 hPa value. However, the 6 hPa $(pd)_{\min}$ estimate is unreliable due to the broad minimum and the Paschen scaling discrepancy discussed in Section 5.2. At 4 hPa, no minimum was observed: the breakdown voltage was still decreasing at the largest accessible gap ($d = 5.5$ mm, $U_{\text{br}} \approx 519$ V), so no γ can be extracted.

6.4 Linear Plot

Figure 4 shows $\frac{d}{U_{\text{br}}}$ plotted against $\ln(d)$ for all three pressures. The linearised Paschen equation predicts straight lines on the right branch (past the minimum) with slope $\frac{1}{Bp}$, from which the gas constant B can be extracted independently. The fitted slopes give B estimates of 235 (8 hPa), 166 (6 hPa), and 226 (4 hPa) $(\text{Pa} \cdot \text{m})^{-1}$, all a factor of 2–3 below the expected value of 487 $(\text{Pa} \cdot \text{m})^{-1}$.

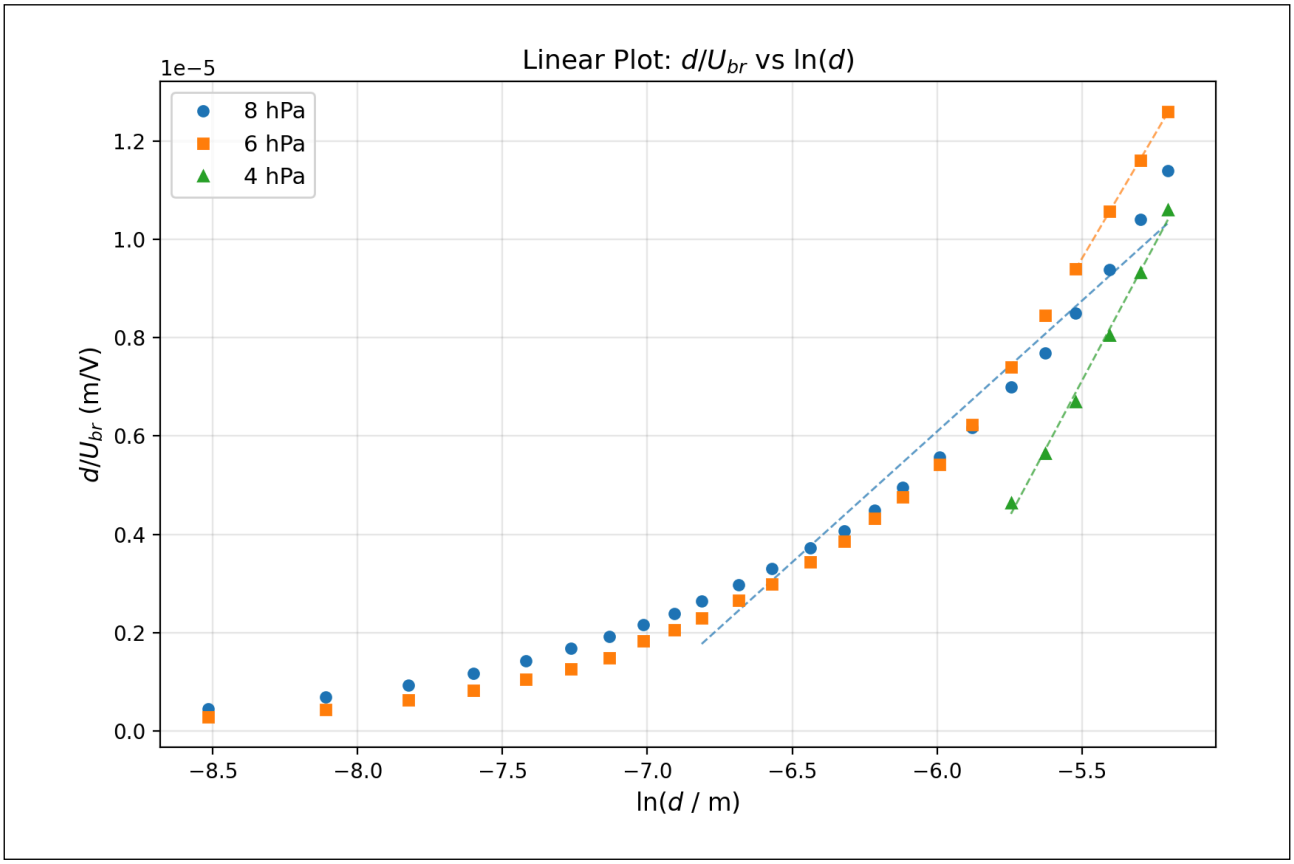

Figure 4: Linear representation: $\frac{d}{U_{\text{br}}}$ vs $\ln(d)$. The dashed lines are least-squares fits to the data past the Paschen minimum.

This poor agreement reflects two compounding effects. First, the limited dynamic range: the right branch of the 8 hPa curve spans only a factor of ≈ 5 in d (from 1.1 to 5.5 mm), over which U_{br} rises gently from 416 to 482 V — a 16% change — so the fit is dominated by the endpoints and sensitive to curvature. Second, the streamer-depressed right branch: because U_{br} is systematically lower than the Townsend prediction at large d, the ratio $\frac{d}{U_{\text{br}}}$ is systematically too high, which steepens the fitted slope and yields a B below the true value. This is consistent with the right-branch departure discussed in Section 5.2.

The intercept extrapolation is even more problematic: $\gamma = \frac{1}{e^C - 1}$, where C is recovered from the intercept, so a modest error in intercept is exponentiated into orders-of-magnitude errors in γ. The γ values extracted from the linear fits (10^{-7} to 10^{-9}) are physically meaningless. The 4 hPa fit is additionally unreliable because the minimum was never reached — all six 4 hPa points lie on the left branch, where the linearisation does not apply. This representation serves as a qualitative consistency check — the data are approximately linear on the right branch — but it is not a reliable route to B or γ with these data.

7 Discussion

7.1 Validity of the Paschen Scaling

The 8 hPa data provide the most complete test of Paschen's law. Near the minimum ($pd \approx 0.5$–1.5 Pa $\cdot$ m), the measured points agree with the theoretical curve ($\gamma = 0.0017$) to within ≈ 10 V. On the right branch, however, the data progressively fall below the Townsend prediction: at $pd \approx 3$ Pa $\cdot$ m the measured voltage is ≈ 130 V below theory, and the discrepancy exceeds 300 V by $pd \approx 4.4$ Pa $\cdot$ m (Figure 3). This right-branch depression is present in all three datasets and is a well-known limitation of the Townsend framework. At high pd, the electron avalanche generates enough space charge to distort the local electric field, and breakdown transitions from the Townsend (avalanche) mechanism to the streamer mechanism, where a self-propagating ionisation front short-circuits the gap at a voltage below the uniform-field Townsend prediction [2]. The Paschen formula (Equation 8) assumes a uniform field and a single secondary-emission feedback loop, so it overestimates the right-branch voltage whenever streamer inception becomes the controlling process.

Within the 6 hPa dataset, there is an additional systematic shift: the 6 hPa points sit 30–50 V below the 8 hPa points at the same pd, and the apparent minimum lies near $(pd)_{\min} \approx 2.4$ Pa $\cdot$ m rather than ≈ 0.88 Pa $\cdot$ m. The $U_{\min}$ values themselves are much closer: 425 V at 6 hPa versus 416 V at 8 hPa, which via Equation 10 correspond to $\gamma \approx 0.0016$ and 0.0019 respectively — only a 15% change. This near-constancy of $U_{\min}$ coupled with a factor-of-3 shift in $(pd)_{\min}$ cannot be explained by electrode ageing alone, since a change in γ would shift both quantities proportionally through the constant C (Equation 9, Equation 10). The additional shift points to a mechanism that depresses the right branch selectively — consistent with the streamer transition occurring at lower pd at 6 hPa (where the lower gas density produces a longer mean free path and allows streamer-favourable avalanche lengths at smaller gap voltages) and with progressive electrode roughening that enhances local field concentration.

Pressure drift is a secondary concern: a 0.5 hPa error in the gauge reading at 6 hPa would shift the pd axis by $\approx 8\%$, far too small to account for the observed departure.

7.2 Trial-to-Trial Scatter

Most data points show excellent reproducibility: at 8 hPa, 16 of 24 gap distances have $\sigma \leq 1$ V across the three trials (Table 1). However, a few points show markedly larger scatter. At $d = 2.0$ mm (8 hPa), the first trial gave 457 V while the second and third gave 439 and 442 V ($\sigma = 9.6$ V). At $d = 4.5$ mm (8 hPa): 473, 488, 476 V ($\sigma = 7.9$ V). At $d = 0.2$ mm (6 hPa): 728, 737, 717 V ($\sigma = 10$ V).

The large-scatter points cluster in two regimes. At the steep left branch (small d, high voltage), the breakdown voltage is highly sensitive to the availability of a seed electron: at high fields the discharge can trigger from a single cosmic-ray-produced electron, and the timing of this event is stochastic. At large d on the right branch, the electrode alignment becomes more critical — a slight tilt of the movable electrode at $d > 4$ mm produces a non-uniform gap, so the discharge initiates at the narrowest point rather than at the nominal d, and which point that is can vary between trials. Both effects are consistent with the manual's advice to increase the voltage slowly (< 1 V/s) near breakdown to improve reproducibility.

7.3 Applications

The Townsend discharge framework has direct engineering relevance. The Paschen minimum for brass electrodes in air, measured here as $U_{\min} \approx 416$ V at $(pd)_{\min} \approx 0.88$ Pa·m, sets the worst-case insulation requirement for any air-insulated gap at this pressure range. Gas-insulated switchgear exploits gases with higher Paschen minima (e.g. SF_6) to reduce the physical clearance needed for high-voltage equipment [2].

7.4 Sources of Uncertainty

The dominant uncertainty is the identification of the Paschen minimum location. At 8 hPa, U_{br} varies by only 2 V between $d = 0.8$ and $d = 1.1$ mm (417 vs 416 V), so the minimum lies somewhere in this range; the discrete 0.1–0.15 mm gap spacing prevents localising it more precisely. This $\delta d_{\min} \approx 0.1$ mm propagates to a $\approx 60\%$ uncertainty in γ when extracted from $(pd)_{\min}$, compared to only $\approx 5\%$ when extracted from $U_{\min}$.

The multimeter's peak-hold function introduces a systematic upward bias if the voltage is ramped too quickly: the recorded peak may exceed the true static breakdown threshold. This effect is most significant on the steep left branch where U_{br} changes rapidly with voltage ramp rate, and less relevant near the minimum where the curve is flat and the ramp was performed slowly.

The pressure gauge resolution (± 0.1 hPa) contributes a $\approx$ 1–2% uncertainty in pd, which is small compared to the other sources but not negligible for the 4 hPa data where $\frac{0.1}{4} = 2.5\%$.

8 Conclusion

The Paschen curves measured for air at 4, 6, and 8 hPa show the expected U-shaped dependence on electrode gap distance. The 8 hPa curve exhibits a clear minimum at $d \approx 1.0$–1.1 mm ($U_{\min} \approx 416$ V), and the Townsend theory matches the data well in the vicinity of this minimum ($pd \approx 0.5$–1.5 Pa · m). From the minimum, the second Townsend coefficient was estimated as $\gamma = 0.0017 \pm 0.0003$, within the expected range for metallic cathodes in air.

On the right branch, all three datasets fall systematically below the Townsend prediction, by up to 300 V at the largest pd values. This is consistent with a transition from the avalanche to the streamer breakdown mechanism at high pd, where the space charge of a sufficiently long avalanche distorts the field and triggers breakdown at a lower voltage than the uniform-field Townsend model predicts. The 6 hPa data exhibit an additional systematic shift: their apparent minimum lies at $(pd)_{\min} \approx 2.4$ Pa · m, nearly three times the 8 hPa value, despite the minimum voltages being similar (425 vs 416 V). This decoupling between $U_{\min}$ and $(pd)_{\min}$ cannot be explained by electrode ageing alone and is better understood as the superposition of streamer effects and progressive electrode roughening on the standard Paschen behaviour. The linearised representation confirms approximate right-branch linearity but yields unreliable quantitative estimates of B and γ, reflecting the limited dynamic range of the data. At 4 hPa, only the descending left branch was accessible.

9 References

1. Plasma Physics Laboratory Manual, Experimental Physics II, NUS (2024).
2. Y. P. Raizer, *Gas Discharge Physics*, Springer (1991).
3. A. N. Tkachev and S. I. Yakovlenko, "The Townsend coefficient and the Paschen law", *Journal of Physics: Conference Series* **44**, 83 (2006).

10 Declaration on the Use of Generative AI

I declare that I **HAVE** used generative AI tools to produce this assignment.

I acknowledge that generative AI was used in the following manner:

AI Tool Used	**My Prompt and AI Output**	**How the Output Was Used**
Claude Code	**Prompt:** "Help me transcribe the handwritten data table, compute Paschen curve averages, generate U_{br} vs d and U_{br} vs pd plots, fit the linear representation, and extract the second Townsend coefficient γ." **Output:** Python script for data processing, plotting, and γ extraction	Used for data transcription assistance and plotting automation. All breakdown voltage measurements were performed by me, and the physical interpretation of the Paschen curves and γ values is my own.
Claude Code	**Prompt:** "Help with Typst formatting for figures, tables, equations, and layout. Check that cross-references and file paths compile correctly." **Output:** Typst formatting guidance and layout suggestions	Used only for formatting. All experiment content, analysis, and scientific interpretations were written and verified by me.

Table 3: AI Tool Usage Declaration